Surface & Coatings Technology 351 (2018) 128–135

Contents lists available at ScienceDirect

Surface & Coatings Technology

journal homepage: www.elsevier.com/locate/surfcoat

Synthesis and characterization of sol-gel derived non-stoichiometric aluminum phosphate coating

F.S. Sayyedan[a,b,*], M.H. Enayati[a], M. Hashempour[b], A. Vicenzo[b], M. Bestetti[b]

[a] Department of Materials Engineering, Isfahan University of Technology, Isfahan 8415683111, Iran
[b] Department of Chemistry, Materials and Chemical Engineering, Politecnico di Milano, 20133, Italy

ARTICLE INFO

Keywords:
Aluminum phosphate
Amorphous-nanocrystalline
Coating
Sol-gel

ABSTRACT

The aim of this study was to synthesize a non-stoichiometric aluminum phosphate coating with high thermal stability. The aluminum phosphate precursor solution, in the presence of polyvinylpyrrolidone (PVP) as a crack-limiting agent was prepared by a sol–gel process and then applied on AISI 304 stainless steel substrate using the dip coating technique. Phase composition analysis of the coating material was performed by X-ray diffraction (XRD). The surface and cross sectional morphology of the coating after annealing at 500 °C for 15 min were observed using scanning electron microscopy (SEM). Topography and roughness of coated surface were investigated by atomic force microscopy (AFM). The amorphous-nanocrystalline structure and distribution of nanocrystals in the amorphous matrix were studied by transition electron microscopy (TEM). Thermal analysis and study of amorphous to crystalline transformation were investigated by thermal-gravimetric and differential scanning calorimetry (TG-DSC). Molecular spectroscopy of the synthesized powder was studied by Raman spectroscopy. According to SEM and AFM images a smooth, uniform, continuous and crack-free coating with 6.7 nm surface roughness was achieved. XRD analysis showed that the amorphous structure of the coating remained almost unchanged after annealing at 500 °C for 15 min. Conversely, an amorphous-nanocrystalline structure was obtained after air annealing at 1100 °C for 1 h. Also, oxide peaks number and intensity after oxidation at 1100 °C for 10 h were remarkably less in the coated sample than the bare one indicating the surface protection of aluminum phosphate coating against oxidation. The presence of graphitic and amorphous carbon (I_D:I_G = 0.97) in the coating structure was confirmed by Raman spectroscopy. TEM observations also confirmed the amorphous structure of the coating after annealing at 500 °C for 15 min and the partial transformation into a mixed amorphous-nanocrystalline structure after annealing at 1100 °C for 1 h. Accordingly, the thermal analysis of the coating material showed that the onset temperature of the amorphous to crystalline transformation was around 1050 °C, a value higher compared to previous reports (below 1000 °C) for the same material.

1. Introduction

Surface protection of engineering parts against oxidation is a key factor to prolong their longevity. In this regard, using a material that is chemically inert with low oxygen permeability and good compatibility with several metals, alloys, and ceramics at high temperatures offers an excellent opportunity [1–3]. One of the compositions having the desired properties of a protective coating is aluminum phosphate ($AlPO_4$). Aluminum phosphate has low density (2.56 g·cm^{-3} for berlinite), high melting temperature (1800 °C) and high hardness (6.5 Mohs). It is also stable at high temperatures; as well being chemically compatible with many metals and most widely used ceramic materials including silicon carbide, alumina, and silica over a moderate range of temperatures. However, it is unsuitable to be used as a high temperature ceramic material due to the large volume change and subsequent stresses induced by the polymorphic transformations (berlinite, tridymite, and cristobalite) [4].

Many efforts have been done over the past few years to synthesize aluminum phosphate with amorphous structure via sol-gel process in order to improve oxidation resistance and thermal stability. Most of them have revealed an amorphous to crystalline transition below 1000 °C. For instance, Campelo et al. [5] synthesized amorphous aluminum phosphate using ammonium dihydrogen phosphate ($NH_4H_2PO_4$(which was fully crystallized at 1000 °C. Liu et al. [6] synthesized aluminum phosphate using aluminum nitrate, phosphoric acid and citric acid ($C_6H_8O_7$) which remained amorphous up to 900 °C. Wang et al. [4] synthesized amorphous aluminum phosphate coating using ethanol, aluminum nitrate nonahydrate ($Al(NO_3)_3{\cdot}9H_2O$) and

* Corresponding author at: Department of Materials Engineering, Isfahan University of Technology, Isfahan 8415683111, Iran.
E-mail address: fs.sayyedan@ma.iut.ac.ir (F.S. Sayyedan).

https://doi.org/10.1016/j.surfcoat.2018.07.086
Received 18 March 2018; Received in revised form 1 July 2018; Accepted 30 July 2018
Available online 31 July 2018

phosphorus pentoxide (P_2O_5). The coating synthesized by Wang et al. started to crystallize at 900 °C.

An amorphous aluminum phosphate composition which is stable over 1000 °C has been developed by Sambasivan et al. [1] with low oxygen diffusivity and desirable corrosion resistance at elevated temperatures, which may provide oxidation protection for metal substrates when deposited as a coating [1, 2].

There are several advantages in using sol-gel method to form thin films. However, the crack formation due to shrinkage during drying and annealing stages and corresponding stress development between the coating and the substrate, sets serious limits to the facile applicability of this approach. To overcome this drawback, using an additive could be helpful. The additives decelerate the condensation reaction and facilitate structural relaxation in the coating. Polyvinylpyrrolidone (PVP, $(C_6H_9NO)_n$) can be considered as an effective additive to restrict the crack formation [7–9]. PVP belongs to organic polymers with amide groups which can hybridize with metalloxane polymers in molecular scale through strong hydrogen bonding between the C═O groups of the PVP and the OH groups of the metalloxane polymers. Such C═O groups can be considered as the capping agent for the OH groups of the metalloxane polymers hindering the condensation reaction and facilitating the structural relaxation [9]. PVP with C═O groups can coordinate metal atoms, offering homogeneity in metal atom distribution in sols and gel films [7].

The aim of the present study was to develop a non-stoichiometric amorphous-nanocrystalline aluminum phosphate coating in the presence of PVP as a crack-limiting agent to achieve minimum cracks and maximum uniformity and oxidation resistance by the simple and low-cost sol-gel process. By controlling the stoichiometry and using a suitable surfactant, a metastable structure with high thermal stability was produced [3].

2. Material and methods

2.1. Substrate preparation

A 1 mm thick AISI 304 stainless steel sheet was cut into samples of 20 × 20 mm^2 using a spark wire machine. The chemical composition of the steel substrate is given in Table 1. The samples were ground to 4000 grit SiC abrasive paper followed by polishing using 0.3 μm alumina slurry. The samples were then degreased ultrasonically in acetone, ethanol and distilled water for 10 min. The substrates were chemically etched in a concentrated acid solution of HCl (37%, Sigma-Aldrich) and H_3PO_4 (85%, Sigma-Aldrich) mixed in equal volume fractions for 5 min in order to create surface micro roughness and improve adhesion of the coating to the substrate.

2.2. Coating preparation

The precursor solution for the synthesis of non-stoichiometric amorphous-nanocrystalline aluminum phosphate coating was prepared by sol-gel method. Aluminum nitrate nonahydrate ($Al(NO_3)_3{\cdot}9H_2O$, Merck, 98.5% purity), phosphorus pentoxide (P_2O_5, Merck, 98% purity) and ethanol (C_2H_5OH, Merck, 99.8% purity) were the starting materials. To synthesize the precursor solution, a specified proportion of $Al(NO_3)_3{\cdot}9H_2O$ and P_2O_5 were dissolved in ethanol. The two solutions were mixed together and stirred for several minutes. Polyvinylpyrrolidone (PVP, Sigma-Aldrich, molecular weight = 10,000) was added to the above solution (a 0.5 M PVP concentration) under stirring until complete dissolution. The resulting solution was then used to coat the stainless steel substrates using a lab-made dip coater at the constant withdrawal rate of 15 mm·min^{-1}. The coated samples were dried in an oven at 65 °C and then annealed in air at 500 °C for 15 min. In addition to the coated samples, a separate batch of the prepared gel was dried at 65 °C for 2 h for complete dehydration, which resulted in a light yellow, fluffy gel. Finally, samples of the dried gel were subjected to annealing in air at 500 °C for 15 min or 1100 °C for 1 h, and collected at the end of the treatment for subsequent characterization.

2.3. Coating characterization

2.3.1. XRD analysis

Phase structure analysis of the synthesized powder and coatings were performed by an X-ray diffractometer (XRD, Philips PW1830) using Ni filtered Cu Ka (lCu Ka = 0.154 nm, radiation at 40 kV and 40 mA) over the 2θ range of 10°–90° (time per step: 0.50 s and step size: 0.02°). Grazing Incidence XRD (GIXRD) scans of the coated samples were collected with a grazing incidence angle of 0.8°. XRD spectra were compared to standards compiled by the Joint Committee on Powder Diffraction and Standards (JCDPS).

2.3.2. AFM studies

Topographic studies on the polished, etched and coated surfaces were carried out by atomic force microscopy (AFM, NT-MDT Solver Pro-M) using silicon cantilevers (CSG 10) with tip radius of 10 nm curvature in contact mode and analyzed by Nova RC1 (1.0.26.1138) and WSxM 5.0 Develop 9.1 software [10]. Evaluation of the surface micro-features was performed based on the deflection related signal images of the AFM. Roughness derived from AFM topographic images was calculated over the sample area of 50 μm × 50 μm.

2.3.3. SEM and GDOES investigations

The Surface and cross sectional morphologies of the coating after annealing at 500 °C for 15 min was studied by scanning electron microscopy (SEM), using a Stereoscan 360 Cambridge instrument. Glow discharge optical emission spectrometry (GDOES, GDA 750 HR) technique operated at 700 V and regulated pressure of 2.3 hPa was performed to assess the composition and thickness of the coating.

2.3.4. TEM studies

The amorphous-nanocrystalline structure of the synthesized powders was studied by transmission electron microscopy (TEM) using a Philips CM200 FEG TEM instrument. The powder sample for TEM observation was prepared by dispersing the powder in methanol and adding a few drops of the suspension on carbon coated TEM grid. Complementary processing of images was carried out by ImageJ where needed.

2.3.5. Thermal analysis

Thermal stability and phase transformations of the dried gel were investigated using a thermo-gravimetric differential scanning calorimetry analyzer (TG-DSC, SETARAM) in the range of 30–1200 °C at a heating rate of 10 °C min^{-1} in air.

2.3.6. Raman spectroscopy

Raman spectroscopy (Horiba Jobin-Yvon LabRam HR-800) was used to study the presence of carbonaceous phases in the synthesized

Table 1
Chemical composition of substrate in terms of weight percent of the elements.

Element	Fe	C	Si	S	P	Mn	Ni	Cr	Mo	Cu	Nb	Ti	V
Wt%	70.52	0.0455	0.295	< 0.030	< 0.007	1.52	11.3	16.0	< 0.050	0.164	0.0705	0.0145	0.0537

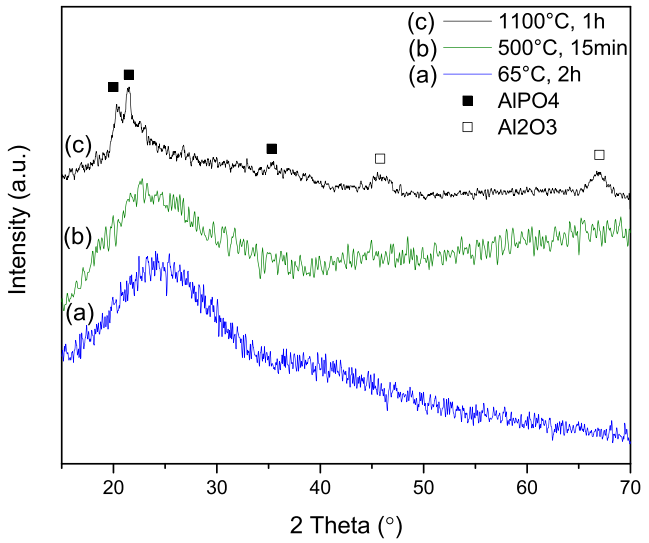

Fig. 1. X-ray diffractograms of the synthesized aluminum phosphate (a) gel dried at 65 °C for 2 h and powder annealed at (b) 500 °C for 15 min and (c) 1100 °C for 1 h.

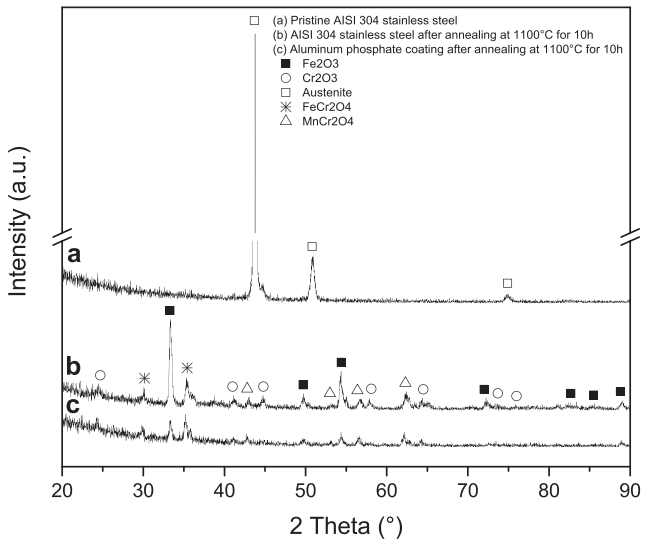

Fig. 2. GIXRD diffractograms of (a) the pristine bare substrate (stainless steel 304), (b) the bare substrate after annealing at 1100 °C for 10 and (c) the aluminum phosphate coating after annealing at 1100 °C for 10 h.

powder calcined at 1100 °C for 1 h. The Raman shift window of 2000–1000 cm^{-1} was investigated using a 514 nm laser excitation with a 0.1 mW power.

3. Results and discussion

3.1. Phase composition analysis

The X-ray diffractograms of the synthesized powder after drying at 65 °C for 2 h, annealing at two different temperatures, namely, 500 °C for 15 min and 1100 °C for 1 h, are shown in Fig. 1.

It is seen that the structure of the synthesized powder evolves by heat treatment. The as-synthesized dried gel does not show any crystalline feature and is characterized by a broad hump at low 2θs (between 20°–30°), indicative of amorphous nature. Calcination at 500 °C does not remarkably modify the pattern, except for the splitting of the board hump in the low angle region and possibly, the appearance of some weak reflections over the amorphous background. Conversely, calcination at 1100 °C clearly promotes the crystallization of the sample as demonstrated by $AlPO_4$ and Al_2O_3 peaks, supposedly embedded in the parent amorphous aluminum phosphate matrix. Since the hump in the low angle diffraction range has not disappeared and crystalline peaks are of very weak intensity, we infer that the structure has a mixed amorphous-nanocrystalline nature.

Fig. 2 illustrates the GIXRD diffractograms of the pristine AISI 304 stainless steel as well as that of the coated sample before and after annealing at 1100 °C for 10 h. The peaks at 44°, 51° and 75° in the pristine sample are related to γ-Fe (austenite) phase in AISI 304 stainless steel [12, 13].

The effect of 10 h oxidation at 1100 °C on the uncoated sample is obvious, as revealed by the formation of a complex scale rich in Fe_2O_3 and incorporating other oxides, such as Cr_2O_3, $MnCr_2O_4$ and $FeCr_2O_4$. The oxide layer is apparently thick since the pattern does not show the reflections from the austenitic substrate. The protective effect of the aluminum phosphate coating against high temperature oxidation can be evaluated by comparing the patterns of coated and uncoated samples. Clearly, oxide peaks number and intensity have remarkably decreased in the coated one. Such capability is attributed to the low oxygen diffusivity in this compound [1]. The peaks present on the coated sample after oxidation are mainly related to Fe_2O_3 and $FeCr_2O_4$. However, minor reflections from Cr_2O_3 and $MnCr_2O_4$ are also present. In addition, no obvious diffraction peak corresponding to $AlPO_4$ can be detected in this sample, which is an indication of the dominant amorphous nature of the coating (though, expectedly, any diffraction peaks due to a small fraction of crystalline $AlPO_4$ would probably be overwhelmed by the amorphous background).

3.2. Micro roughness investigation

Fig. 3 shows the AFM images of the substrate surface after polishing by 0.3 μm alumina slurry (Fig. 3a and b), of the same after etching in a concentrated acid solution of HCl 37% and H_3PO_4 85% mixed in equal volume fractions for 5 min (Fig. 3c and d) and after coating and annealing at 500 °C for 15 min (Fig. 3e and f). Fig. 3a and b present a smooth surface while Fig. 3c and d show a uniform roughening of the surface upon etching, which helps improving wettability and adhesion of the coating to the substrate. The roughness value of the etched surface (7.2 nm) is six times greater than that for the polished surface (1.2 nm). The roughness of the surface is slightly decreased, namely from 7.2 nm to 6.7 nm, after coating with aluminum phosphate (Fig. 3e and f). Sambasivan et al. [3] reported the surface roughness values of uncoated and aluminum phosphate coated Inconel substrate using atomic force microscopy. The root mean square roughness of the uncoated and aluminum phosphate coated surface was 57.9 nm and 14.5 nm, respectively. The surface roughness was decreased by four times after coating. They called this behavior as “planarization effect”. For many applications including tribological uses and wear concerns, decreasing surface roughness may be important [11]. In the present case, the remarkably lower roughness of the pristine surface did not allow to highlight this effect of the coating.

3.3. Microstructure analysis

Fig. 4 exhibits the SEM micrographs and GDOES analyses of the amorphous aluminum phosphate coating formed on stainless steel 304 after annealing at 500 °C for 15 min.

Preferential etching of the grain boundaries is immediately evident from Fig. 4a and b. As seen in SEM micrographs of dried (Fig. 4a and b) and annealed (Fig. 4c and d) samples, the coating is uniform and continuous. Moreover, except near the edges of the sample, where a greater accumulation of the solution occurred, we could detect only occasionally cracking defects in the central regions. In this respect, we

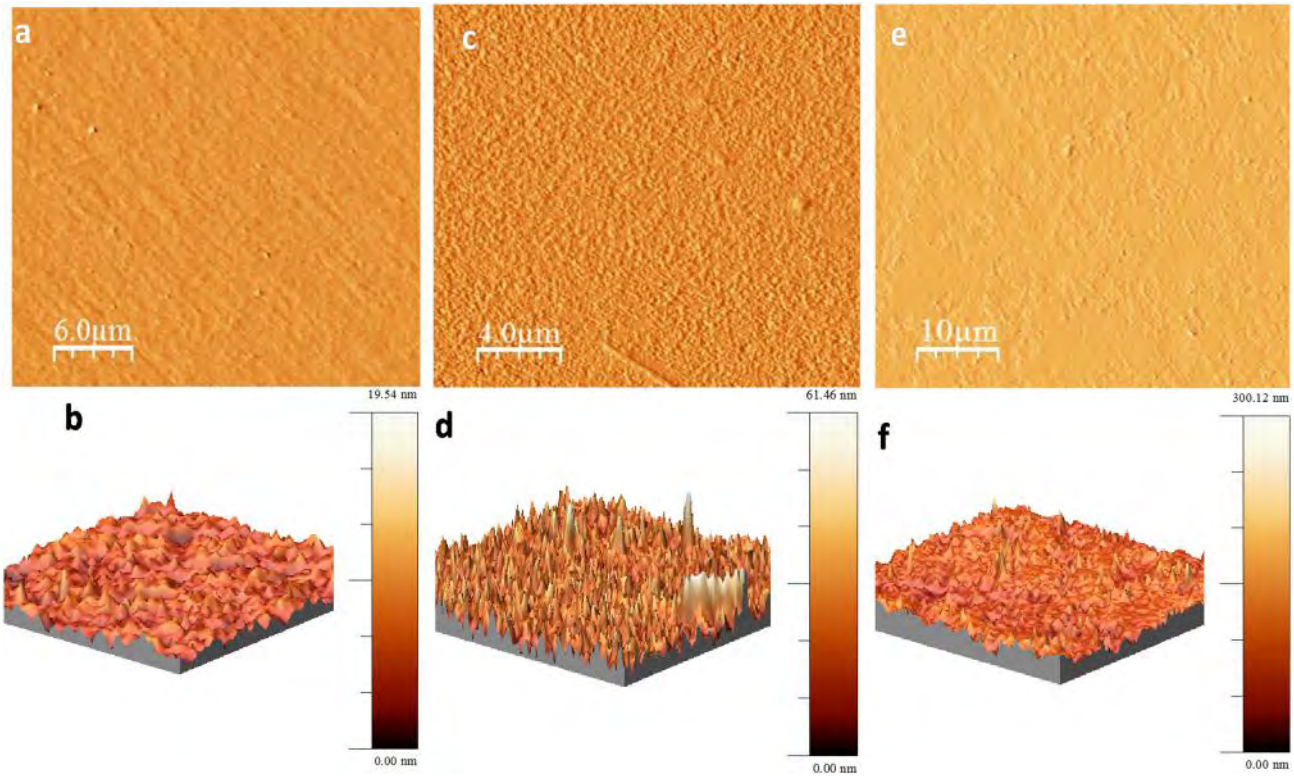

Fig. 3. (a) Deflection mode of polished surface of the substrate (b), 3D image of (a), (c) Deflection mode of polished and etched surface of the substrate, (d) 3D image of (c), (e) Deflection mode of polished and etched and coated surface with aluminum phosphate after annealing at 500 °C for 15 min, (f) 3D image of (e).

emphasize that in order to achieve such level of coating integrity, we studied in detail and tuned a wide range of parameters pertaining to both sample preparation and sol-gel composition. In particular, controlled roughness of the specimens, fine-tuned content of the PVP additive, and careful selection of the heating and cooling rates during annealing, were some of the most important parameters strongly contributing to the obtainment of a nearly crack-free coating.

Line profile analysis of the film performed by GDOES, as shown in Fig. 4e, is meaningful in revealing a surface enrichment by aluminum, phosphorous and oxygen, as the decaying trend for these elements suggest, and in providing direct evidence of the film thickness being around 200 nm. Namely, the assessment of the thickness is inferred from the fact that line profiles for the steel alloy components show all a sharply rising trend initiating at about 200 nm depth, concomitantly with a distinct downward step in the line profile of aluminum.

Fig. 4f shows the cross-sectional microstructure of the coating after annealing at 500 °C for 15 min. It can be found that the coating is dense, uniform, with good adhesion to the substrate.

Film stability under thermal cycling conditions is critically important for many applications and the thin nature of these films will help to minimize the residual thermal stresses such that cracking and spallation is prevented [3].

3.4. Raman spectroscopy

The presence of amorphous carbon in the surface region of the coating material was further investigated by Raman spectroscopy. Fig. 5 shows the Raman spectrum of the synthesized aluminum phosphate powder calcined at 1100 °C for 1 h. The peaks at 1350 cm^{-1} and 1600 cm^{-1}, corresponding to the D and G band regions of carbon, respectively, and their relative intensity (I_D:I_G = 0.97), suggest the presence of either amorphous or turbostratic graphitic carbon in the structure of aluminum phosphate as also evidenced in earlier reports [14]. The source of carbon can be attributed to the ethanol and PVP used during synthesis of the precursor sol.

3.5. Thermal analysis

The TG-DSC trace of aluminum phosphate gel dried at 65 °C for 2 h is shown in Fig. 6. The endothermic peak around 150 °C with 51% weight loss is related to the evaporation of residual moisture and the structural water of aluminum nitrate nonahydrate [4, 15].

Decomposition of aluminum nitrate is reported to occur at temperature in the range of 150–250 °C [15–17]. The process of thermal decomposition of hydrated aluminum nitrate comprises a series of simultaneous reactions such as dehydration, hydrolysis, formation of hydroxyl salts and their dihydroxylation [18]. The exothermic peak at 250 °C with 6% weight loss is attributed to the thermal decomposition of residual nitrate and the gas escape of nitrogen oxides [16]. Al $(NO_3)_3{\cdot}9H_2O$ is decomposed to the corresponding oxides according to reaction (1) [15].

$$Al(NO_3)_3{\cdot}9H_2O \rightarrow Al(NO_3)_3 \rightarrow \frac{1}{2}A1_2O_3 + \frac{3}{2}NO_2 + \frac{3}{2}O_2 \quad (1)$$

It is worth noting that the $A1_2O_3$ formed in reaction (1) is amorphous. Melnikov et al. [18] studied the high temperature X-ray diffractograms of aluminum nitrate octahydrate ($Al(NO_3)_3{\cdot}8H_2O$). They reported that at temperature of 150 °C, or probably lower, original nitrate hydrate is completely transformed into amorphous material characterized by typical diffraction halos. They realized that even at 300 °C no crystalline Al_2O_3 phase could be detected, probably due to a slow kinetics. It is not surprising because in the case of a related iron nitrate the diffraction peaks of Fe_2O_3 were observed only after heating the compound for four days [18].

The weak exothermic peak at 350 °C with 4% weight loss is related to the oxidation of hydrocarbons associated with ester groups [2, 19]. There are no further exothermic features in the thermogram up to 1050 °C suggesting that an insignificant portion of carbon burns up to

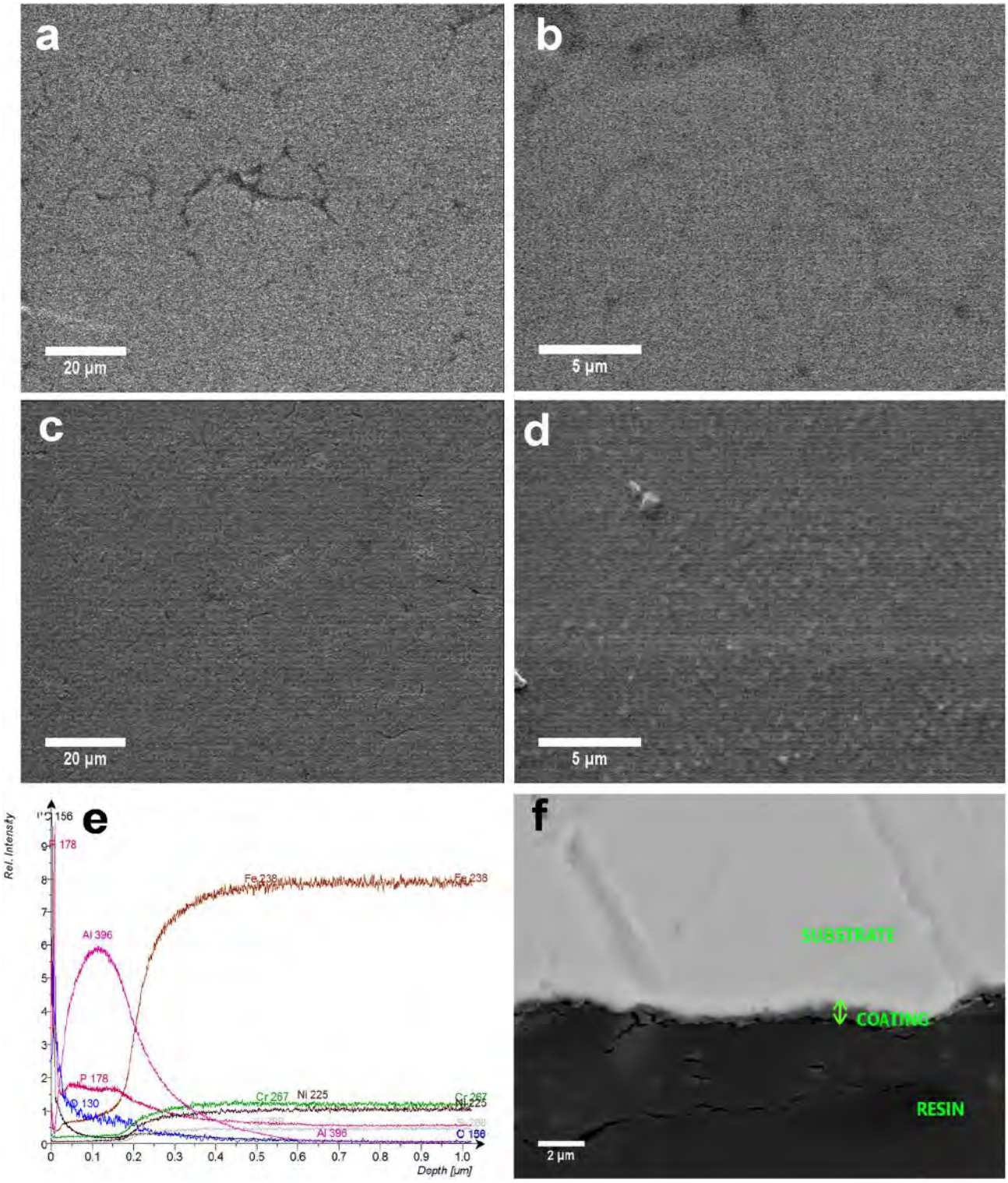

Fig. 4. Surface and cross-sectional image and GDOES analyses of the amorphous aluminum phosphate coating formed on stainless steel 304 after drying and annealing steps: (a) and (b) surface morphology after drying at 65 °C for 2 h at two different magnifications, (c) and (d) surface morphology after annealing at 500 °C for 15 min at two different magnifications, (e) GDOES analysis after annealing at 500 °C for 15 min, (f) Cross section morphology of coating after annealing at 500 °C for 15 min.

350 °C and the remaining carbonaceous materials in the matrix are stable even over 1000 °C in air [2, 14]. This observation, together with the result of Raman spectroscopy of the aluminum phosphate powder after annealing at 1100 °C for 1 h (Fig. 5), strongly suggest the entrapment of carbon particles in the inorganic matrix.

The weak exothermic peak at 1050 °C corresponds to the nucleation of nanocrystals of $AlPO_4$ and Al_2O_3 according to the X-ray diffractograms given in Fig. 1c. TEM observations presented in the next section also confirmed the presence of these nanocrystals in the amorphous matrix.

The synthesized aluminum phosphate in this research, unlike common aluminum phosphates (berlinite) contains Al—O—Al groups

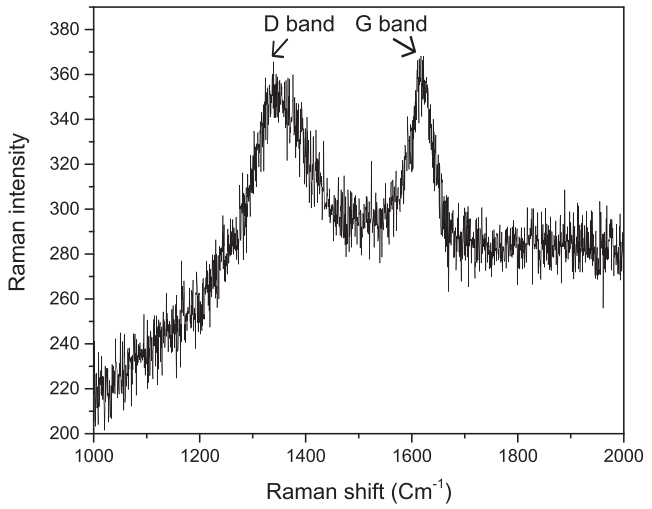

Fig. 5. Raman spectra of the synthesized aluminum phosphate powder annealed at 1100 °C for 1 h.

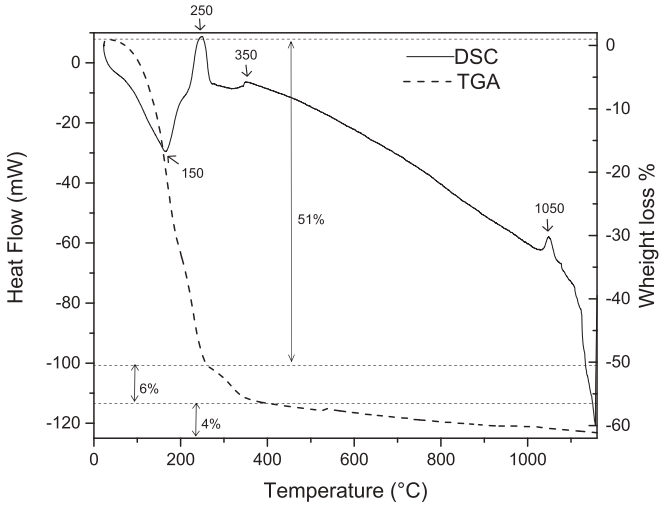

Fig. 6. TG-DSC trace of the synthesized aluminum phosphate gel dried at 65 °C for 2 h.

besides Al—O—P groups directly bonded to Al—O—P groups. These [P—O—Al—O—Al] linkages can exit in the precursor solution or can be formed during heat treatment. In fact, the majority of excess aluminum species that are not directly bonded to P—O groups are linked to the aluminum of the ester complex in the precursor solution. Presence of such "interrupting" Al—O—Al groups in a continuous network containing Al-O-P linkages resist the nucleation of both crystalline $AlPO_4$ and Al_2O_3, thus retaining the amorphous character to elevated temperatures (even over 1000 °C). The thermal stability is extended to higher temperatures with increasing amount of excess aluminum in the precursor solution [1].

3.6. TEM investigations

TEM bright field images and selected area electron diffraction (SAED) patterns of aluminum phosphate gel dried at 65 °C for 2 h, annealed at 500 °C for 15 min and at 1100 °C for 1 h, are shown in Fig. 7.

The gel dried at 65 °C is composed of micrometer scale particles (Fig. 7a) of irregular shape, suggestive of the amorphous nature of the material.

High resolution TEM (HRTEM) analysis of this sample (Fig. 7b) confirms the lack of crystallinity, as revealed by the absence of atomic fringes, in addition showing the presence of smaller constituents, supposedly, aggregated products of sol-gel, in the big particles. Expectedly, the SAED pattern of this sample (Fig. 7c), as well as the diffraction pattern intensity profile (Fig. 7j) do not show any crystalline features. The sample annealed at 500 °C, in contrast to the dried gel, shows clear and distinct particles (Fig. 7d) with almost the same size as the dried gel. Annealing caused the decomposition of volatile residues of the sol-gel process, such as nitrates and organics, leading to a clear observation of the powder particles. Nevertheless, HRTEM image of this sample (Fig. 7e) as well as its SAED (Fig. 7f) do not show signs of crystallinity. The diffraction pattern intensity profile of this sample (Fig. 7j) shows slight variation with respect to the dried gel, by minor shift of the broad intensity peaks to lower scattering vectors. Although this confirms an influence of the annealing treatment at 500 °C on the structure of the material, the extent of its modification is apparently small. Fig. 7g and h show the products of calcination at 1100 °C, demonstrating strong changes in the appearance of the powders both at micro- and nano-scale observations, respectively. The low magnification TEM image in Fig. 7g shows that the relatively large particles seen in 500 °C annealed sample (Fig. 7d) appear separated into small fragments (Fig. 7g) probably due to stresses induced by the formation of crystalline phases. Whereas the annealed powder at 500 °C possessed an approximate particle size of 0.5–1 μm, after calcination at 1100 °C, this approximate particle size reduces to 200 ± 50 nm. Moreover, HRTEM (Fig. 7h) as well as dark field HRTEM images (not shown here) demonstrate the presence of tiny nanocrystals in the size range of 2–10 nm, embedded in the matrix of the larger particles. These could be either Al_2O_3 nanoparticles crystallized at high temperature due to the presence of excess aluminum in the sol-gel precursor, or even, $AlPO_4$ crystallites separated from the amorphous matrix. SAED image of this sample (Fig. 7i) clearly reveals crystalline rings and spots that when looked at in the diffraction pattern intensity profile (Fig. 7j), demonstrated the presence of both Al_2O_3 and $AlPO_4$.

4. Conclusions

Aluminum phosphate thin film was applied on AISI 304 stainless steel by means of a simple dip coating technique successfully. XRD analysis confirmed that the sol-gel product is completely amorphous and transforms to amorphous-nanocrystalline structure after annealing at 1100 °C for 1 h. According to SEM and AFM images, a smooth, uniform, continuous and nearly crack-free coating with 6.7 nm surface roughness was obtained. Raman spectroscopy showed the presence of graphitic and amorphous carbon in the amorphous aluminum phosphate matrix. Thermal analysis of the coating material showed that the onset temperature of the amorphous to crystalline transformation with 10 °C·min^{-1} was around 1050 °C. TEM observations confirmed the formation of an amorphous-nanocrystalline structure after annealing at 1100 °C for 1 h, which includes nano-sized crystalline particles of 200 ± 50 nm in an amorphous matrix. The protective effect of the aluminum phosphate coating against high temperature oxidation at 1100 °C was revealed by majority of hematite peaks in the X-ray diffractogram of the un-coated substrate compared to that of the aluminum phosphate coated one. It is expected that the synthesized coating protects metal/alloy surfaces against oxidation at high temperatures (over 1000 °C).

Acknowledgments

The authors hereby sincerely appreciate Professor Nora Francesca Maria Lecis from Department of Mechanics, Politecnico di Milano, for her generous supports on this research. F.S. Sayyedan and M.H. Enayati also gratefully acknowledge the support of the Iran National Science Foundation (INSF) on this research under grant number 94016469.

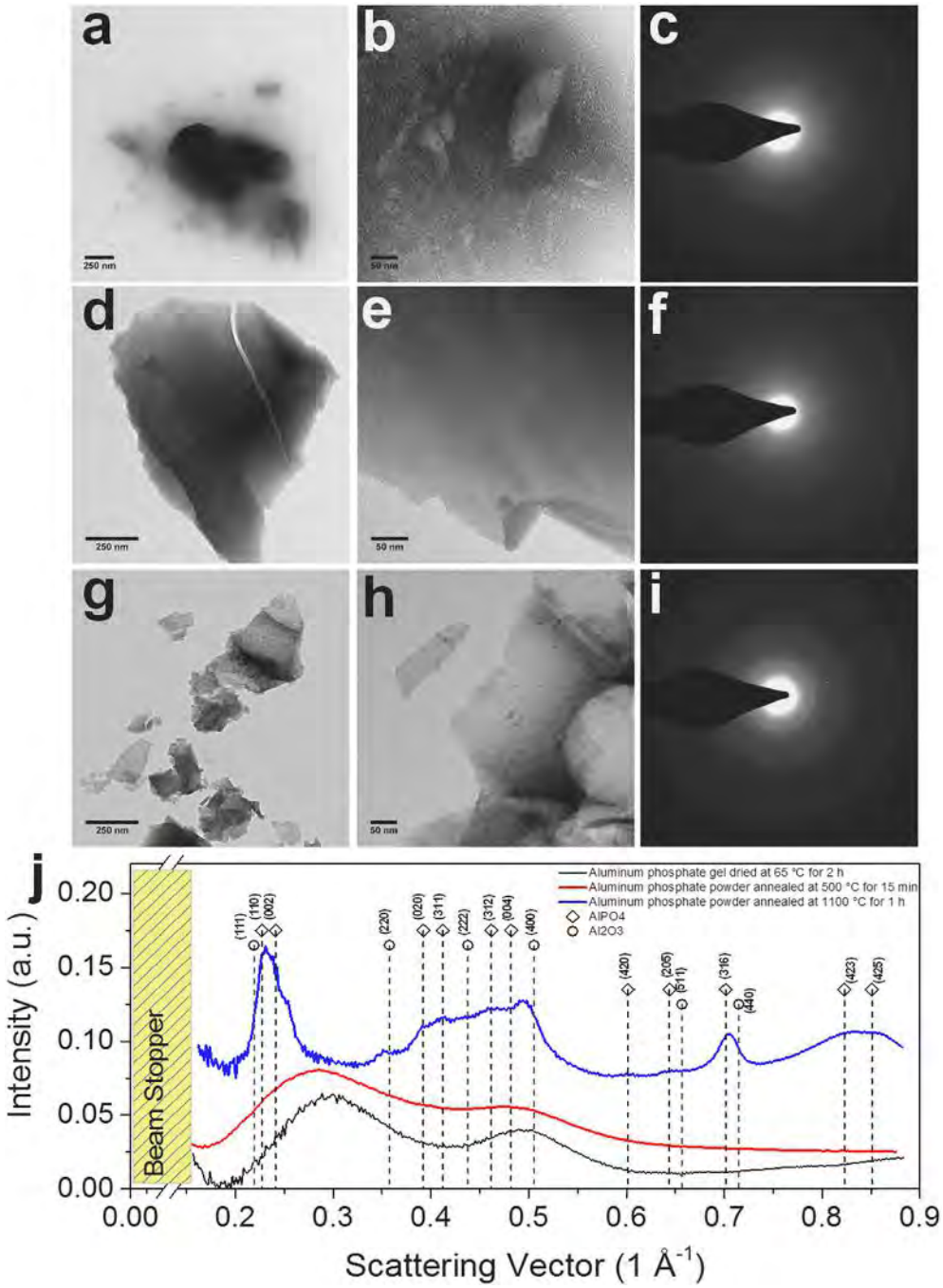

Fig. 7. (a) TEM, (b) HRTEM and (c) SAED of aluminum phosphate gel dried at 65 °C, (d) TEM, (e) HRTEM and (f) SAED of aluminum phosphate powder annealed at 500 °C for 15 min, (g) TEM, (h) HRTEM and (i) SAED of aluminum phosphate powder calcined at 1100 °C for 1 h, and (j) diffraction pattern intensity profile of the three samples.

References

[1] S. Sambasivan, K.A. Steiner, High Temperature Amorphous Composition Based on Aluminium Phosphate, U.S. Patent No. 0011245 A1, Chicago, (2004).

[2] S. Sambasivan, K. Rangan, Aluminium Phosphate Based Microspheres, U.S. Patent No. 7,833,342 B2, Chicago, (2010).

[3] S. Sambasivan, K.R. Steiner, K. Rangan, Aluminum Phosphate Coatings, U.S. Patent No. 7,311,944 B2, Chicago, (2007).

[4] Y.M. Wang, H. Tian, L.X. Guo, J.H. Ouyang, Y. Zhou, D.C. Jia, Amorphous $AlPO_4$ coating formed on titanium alloy for high temperature oxidation protection: oxidation kinetics and microstructure, Surf. Coat. Technol. 252 (2014) 134–141.

[5] J.M. Campelo, M. Jaraba, D. Luna, R. Luque, J.M. Marinas, A.A. Romero, Effect of phosphate precursor and organic additives on the structural and catalytic properties of amorphous mesoporous $AlPO_4$ materials, Chem. Mater. 15 (2003) 3352–3364.

[6] G. Liu, M. Jia, Zh. Zhou, W. Lei, W. Zhang, D. Jiang, Synthesis and pore formation study of amorphous mesoporous aluminophosphates in the presence of citric acid, J. Colloid Interface Sci. 302 (2006) 278–286.

[7] H. Kozuka, S. Takenaka, H. Tokita, M. Okubayashi, PVP-assisted sol-gel deposition of single layer ferroelectric thin films over submicron or micron in thickness, J. Eur. Ceram. Soc. 24 (2004) 1585–1588.

[8] Y. Chen, W. Wei, Formation of mullite thin film via a sol-gel process with polyvinylpyrrolidone additive, J. Eur. Ceram. Soc. 21 (2001) 2535–2540.

[9] H. Kozuka, M. Kajimura, Single-step dip coating of crack-free $BaTiO_3$ films > 1 μm thick: effect of poly(vinylpyrrolidone) on critical thickness, J. Am. Ceram. Soc. 83 (2000) 1056–1062.

[10] I. Horcas, R. Ferna'ndez, J.M. Go'mez-Rodrı'guez, J. Colchero, J. Go'mez-Herrero, A.M. Baro, WSXM: a software for scanning probe microscopy and a tool for nanotechnology, Rev. Sci. Instrum. 78 (2007) 1–8.

[11] B. Tlili, A. Barkaoui, M. Walock, Tribology and wear resistance of the stainless steel. The sol–gel coating impact on the friction and damage, Tribol. Int. 102 (2016) 348–354.

[12] Ch. Kuo, Ch. Lin, G. Lai, Y. Chen, Y. Chang, W. Wu, Characterization and

mechanism of 304 stainless steel vibration welding, Mater. Trans. 48 (2007) 2319–2323.
[13] Ch. Quan, Y. He, Properties of nanocrystalline Cr coatings prepared by cathode plasma electrolytic deposition from trivalent chromium electrolyte, Surf. Coat. Technol. 269 (2015) 319–323.
[14] S. Roy, S. Rangaswamy Reddy, P. Sindhuja, D. Das, V.V. Bhauprasad, $AlPO_4$-C composite coating on Ni-based super alloy substrates for high emissivity applications: experimentation on dip coating and spray coating, Def. Sci. J. 66 (2016) 425–433.
[15] E. El-Shereafy, M.M. Abousekkina, A. Mashaly, M. EI-Ashry, Mechanism of thermal decomposition and γ-pyrolysis of aluminum nitrate nonahydrate $[Al(NO_3)_3{\cdot}9H_2O]$, J. Radioanal. Nucl. Chem. 237 (1998) 183–186.
[16] N. Li, M. Zhong, Z.H. Xu, Z.H. Zhang, Polyesterification synthesis of amorphous aluminum phosphate thermal radiation material with high infrared emissivity, Mater. Lett. 213 (2018) 335–337.
[17] S.H. Yuvaraj, L. Fan-Yuan, C.H. Tsong-Huei, Ye Chuin-Tih, Thermal decomposition of metal nitrates in air and hydrogen environments, J. Phys. Chem. B 107 (2003) 1044–1047.
[18] P. Melnikov, V.A. Nascimento, I.V. Arkhangelsky, L.Z. Zanoni Consolo, Thermal decomposition mechanism of aluminum nitrate octahydrate and characterization of intermediate products by the technique of computerized modeling, J. Therm. Anal. Calorim. 111 (2013) 543–548.
[19] E. Illekova, K. Csomorova, Kinetics of oxidation in various forms of carbon, J. Therm. Anal. Calorim. 80 (2005) 103–108.